Rare Metal Materials and Engineering
Volume 45, Issue 11, November 2016
Online English edition of the Chinese language journal

Available online at www.sciencedirect.com
ScienceDirect

Cite this article as: Rare Metal Materials and Engineering, 2016, 45(11): 2818-2822.

ARTICLE

Improvement of the Corrosion Resistance of Steel Wires by Manufacturing Continuous Bulk Metallic Glass-Coated Steel Wires

Zhang Baoyu[1], Guo Xinge[2], Chen Xiaohua[3], Yang Wenzhi[1], Chen Ziming[1], Huang Wei[1], Shang Fujun[1], Shi Honggang[1]

[1] Ningbo Branch of China Academy of Ordnance Science, Ningbo 315103, China; [2] Institute of Solid State Physics, Chinese Academy of Sciences, Hefei 230031, China; [3] State Key Laboratory for Advanced Metals and Materials, University of Science and Technology Beijing, Beijing 100083, China

Abstract: To improve the corrosion resistance of steel wires, a uniform thin layer of bulk metallic glass alloy with different compositions of $(Zr_{41.2}Ti_{13.8}Cu_{12.5}Ni_{10}Be_{22.5})_{100-x}Nb_x$ (x=0, 3, 5, 8 at%) was coated on the surface of Q195 steel wires by a newly developed continuous coating process. Phase analysis results show that the coating is mainly composed of metallic glass alloy and some other intermetallics. The potentiodynamic polarization tests indicate that the steel wires with metallic glass coating show passivation behavior, and have higher pitting potential and lower corrosion current density than Q195 steel wires. With the increment of Nb content, the passivation region of the metallic glass-coated steel wires become wider while pitting potential is increased. As shown in composition analysis results, it may be attributed to the addition of Nb which has properties of easy passivation and stabilizing the passivation elements of Zr and Ti.

Key words: steel wires; bulk metallic glasses; coatings; pitting corrosion resistance

Bulk metallic glasses (BMGs) are of great interest for their excellent mechanical, physical and chemical properties [1-3]. Compared with their crystalline counterparts, BMGs possess disorder structure, homogeneous components, more easily passivation nonferrous metal elements and eliminate grain boundaries as well as composition segregation, etc. So BMGs show better corrosion resistance than metallic crystal materials counterparts in corrosion environment.

Zr- [4,5], Cu-[6,7], Ti-[8] and Fe-[9] based BMGs possess excellent glass forming ability (GFA), high mechanical properties and high passivation ability in halide-free electrolytes. In contrast, these alloy systems show poor pitting corrosion resistance in aqueous solution containing chlorides ions[10-14]. Many methods have been reported to improve the anti-pitting corrosion ability of metallic glass alloys, such as ion implantation[15], shot peening[16,17], addition of Nb or Ta[18,19].

Recently, more and more attention is paid to the applications of BMG alloys as corrosion resistant coating. On one hand, new systems of bulk BMG have been trapped into difficulty; On the other hand, metallic glass is an ideal candidate for anticorrosion coating because of its excellent wear or corrosion resistance. Fe-[20-24], Zr-[25-27], Ti-[28,29], Cu-[30] based metallic glass alloys are coated on bulk alloy plates by pulse magnetron sputtering, shroud plasma spraying, or pulse laser deposition, thermal spraying, or electrospark deposition. However, only a few studies[31] have been reported on coating metallic glass on metallic wires, which play a key role in transferring loads and power. In our early works[32-37], a newly developed continuous coating technique was developed, which can achieve both higher coating efficiency and lower preparation cost than any other coating process. In order to improve the corrosion resistance of steel wires, a series of

Received date: November 10, 2015
Corresponding author: Zhang Baoyu, Ph. D., Assistant Researcher, Ningbo Branch of China Academy of Ordnance Science, Ningbo 315103, P. R. China, Tel: 0086-574-87017901, E-mail: byzhang@outlook.com

$(Zr_{41.2}Ti_{13.8}Cu_{12.5}Ni_{10}Be_{22.5})_{100-x}Nb_x$ (x=0, 3, 5, 8 at%) BMG-coated Q195 steel wires were prepared by the newly developed continuous coating process. And their corrosion behavior in 3.5 wt% NaCl aqueous solution was studied using potentiodynamic polarization tests combined with scanning electron microscopy and energy dispersive spectrometer.

1 Experiment

Master alloy ingots with nominal composition of $(Zr_{41.2}Ti_{13.8}Cu_{12.5}Ni_{10}Be_{22.5})_{100-x}Nb_x$ (x=0, 3, 5, 8, at%) were synthesized by arc-melting pure metal blocks under a Ti-gettered argon atmosphere. Nb and Zr were first melted as master alloy and then were remelted with other metallic elements for four times to ensure the homogenization of the refractory Nb in the alloy. The surface of Q195 steel wire with diameter of 0.5 mm was polished using 12 μm SiC sandpapers and then cleaned in the solution of acetone and ethanol. Then the metallic glass alloy was coated on the surface of the Q195 steel wire by the continuous coating process. A Q195 steel wire was firstly drawn through a crucible filled with the melting metallic glass alloy, and then quickly entered the cooling unit to obtain metallic glass coating. More details of this coating process can be referred to Refs. [32-37].

Phase analysis of the metallic glass-coated steel wires was performed using Rigaku D/max-rB type of X-ray diffraction (XRD) with Cu Kα radiation. A row of metallic glass-coated steel wires with length of 16 mm were arrayed on the groove of glass slide, and the XRD patterns reflected the structure information of both the BMG coating and the Q195 steel wire. The pitting corrosion behavior of all BMG-coated steel wires in the 3.5 wt% NaCl aqueous solution was evaluated using model Gill AC manufactured by ACM Instrument. A symbolic three electron cell using a platinum counter electrode and a saturated calomel reference electrode (SCE) was used in the electrochemical polarization tests. The open circuit potential (OCP) measurement was maintained until the potential value change was no more than 2 mV/5 min. The potentiodynamic polarization tests were performed from –100 mV (*vs*. SCE) to +700 mV (*vs*. SCE) with a scanning rate of 10 mV/min. The corrosion potential (E_{corr}), the corrosion current density (I_{corr}) and the pitting potential (E_{pit}) were calculated by Tafel equation method. The surface morphology of the metallic glass-coated steel wires after potentiodynamic polarization tests was observed by scanning electron microscopy (SEM) and the elements distribution in the pitting holes were analyzed by Energy Dispersive Spectrometer (EDS) using a Carl Zeiss Auriga Crossbeam Workstation.

2 Results and Discussion

2.1 Microstructure of the metallic glass-coated steel wire

The cross-section image of $Zr_{41.2}Ti_{13.8}Cu_{12.5}Ni_{10}Be_{22.5}$ (Vit 1)-coated Q195 steel wire is displayed in Fig.1. The metallic glass with thickness of 5~7 μm is uniformly coated on the surface of Q195 steel wire. It is also noticed that most metallic glass coatings strongly bond with the surface of Q195 steel wire. In the left section of Fig.1, there are some micropores near the interface between metallic glass coating and Q195 steel wire, indicating that some gas molecules are trapped during solidification of metallic glass. These gas voids can be eliminated through optimizing the preparation process in further research.

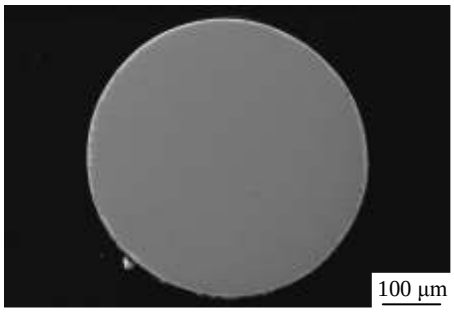

Fig.1 Cross-section photograph of $Zr_{41.2}Ti_{13.8}Cu_{12.5}Ni_{10}Be_{22.5}$ BMG-coated Q195 steel wire

2.2 Phase structure analysis

The XRD patterns of Q195 steel wire and $(Zr_{41.2}Ti_{13.8}Cu_{12.5}Ni_{10}Be_{22.5})_{100-x}Nb_x$ (x=0, 3, 5, 8, at%) BMG-coated steel wires are shown in Fig.2. The patterns of metallic glass-coated steel wires show a wide dispersion of the diffuse scattering peak, which is the characteristic of amorphous structure, superimposed by crystalline diffraction peaks of the Q195 steel wire and some other phases ($Fe_{37}Nb_9Zr_{54}$, Ni_2Zr_3 and NiZr). With the increment of Nb content, the peak intensity of Q195 steel wire decreases while the peak intensity of $Fe_{37}Nb_9Zr_{54}$ increases notably. It is also noticed that the $(Zr_{41.2}Ti_{13.8}Cu_{12.5}Ni_{10}Be_{22.5})_{95}Nb_5$-coated Q195 steel wire contains crystalline phase NiZr.

2.3 Electrochemical analysis

Fig.3 shows the potentiodynamic polarization curves of $(Zr_{41.2}Ti_{13.8}Cu_{12.5}Ni_{10}Be_{22.5})_{100-x}Nb_x$ BMG-coated steel wires

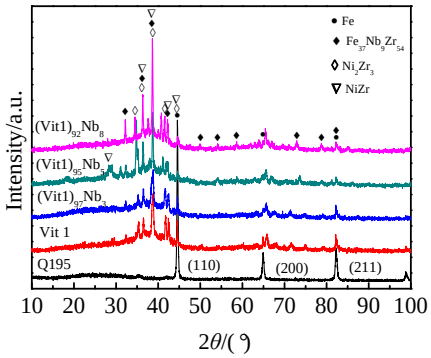

Fig.2 XRD patterns of Q195 steel wire and $(Zr_{41.2}Ti_{13.8}Cu_{12.5}Ni_{10}Be_{22.5})_{100-x}Nb_x$ (x=0, 3, 5, 8, at%) BMG-coated Q195 steel wires

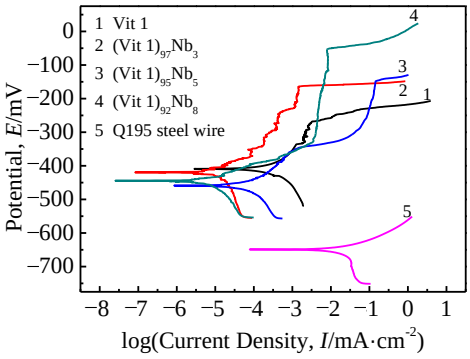

Fig.3 Potentiodynamic polarization curves of $(Zr_{41.2}Ti_{13.8}Cu_{12.5}Ni_{10}Be_{22.5})_{100-x}Nb_x$ BMG-coated steel wires with Nb content of 0at%, 3at%, 5at%, 8at%, in 3.5% NaCl aqueous solution along with Q195 steel wire for comparison

with 0at%, 3at%, 5at% and 8at% Nb content along with that of the Q195 steel wire for comparison. Seen from the bottom right section of Fig.3, the corrosion current density of the Q195 steel wire soon reaches 1 mA/cm^2 after the anode polarization process starts. In contrast to Q195 steel wire, all metallic glass-coated steel wires show obvious passivation regions upon anodic polarization with passive current density lower than 1 μA/cm^2, which is comparable to the results of the monolithic BMG sample and metallic glass-coated steel wires in our early works[33]. The results of potentiodynamic polarization measurements are summarized in Table 1. With the increment of Nb content, the pitting potential and the passivation region of metallic glass-coated steel wires are increased from –268, 141 mV to –52, 394 mV, respectively, while the corrosion current density is decreased from 3.71×10^{-4} to 9.86×10^{-6} mA/cm^2. It is also noticed from Fig.3 that $(Zr_{41.2}Ti_{13.8}Cu_{12.5}Ni_{10}Be_{22.5})_{95}Nb_5$-coated Q195 steel wire shows characteristics of two-step passivation behavior, which is different from the passivation behavior of other metallic glass-coated steel wires. It may be attributed to crystalline phase NiZr, which is shown in Fig.2. During the anode passivation process, second passivation behavior occurs after breaking local passivation film where the metallic glass coating contains crystalline phase NiZr.

2.4 Surface morphologies after polarization

Fig.4 shows the surface morphologies of $(Zr_{41.2}Ti_{13.8}Cu_{12.5}Ni_{10}Be_{22.5})_{100-x}Nb_x$ BMG-coated Q195 steel wires after potentiodynamic polarization tests. It can be seen from Fig.4a that $Zr_{41.2}Ti_{13.8}Cu_{12.5}Ni_{10}Be_{22.5}$-coated Q195 steel wires shows the characteristic of uniform pitting corrosion and the pitting holes uniformly distribute on the whole surface of the $Zr_{41.2}Ti_{13.8}Cu_{12.5}Ni_{10}Be_{22.5}$-coated steel wire. With increasing the Nb content, pitting holes on the surface of metallic glass-coated steel wires decrease in quantity, indicating that the resistance of pitting corrosion is improved. The pitting holes mainly distribute on the lower section of $(Zr_{41.2}Ti_{13.8}Cu_{12.5}Ni_{10}Be_{22.5})_{95}Nb_5$-coated steel wire, which may be related to the local distribution of crystalline phase NiZr. The $(Zr_{41.2}Ti_{13.8}Cu_{12.5}Ni_{10}Be_{22.5})_{92}Nb_8$-coated steel wire shows the best resistance of pitting corrosion. Only a few pitting holes can be observed on the surface of the $(Zr_{41.2}Ti_{13.8}Cu_{12.5}Ni_{10}Be_{22.5})_{92}Nb_8$-coated steel wire, which is in agreement with the result of potentiodynamic polarization tests.

2.5 EDS analysis

To probe the alloying mechanism of passivation films of metallic glass-coated steel wires, local chemical composition distribution of the pitting holes was analyzed using EDS. It can be seen from Fig.5 that the chemical elements concentration of the pitting holes shows an obvious difference between each other. With the Nb content increasing from 0 to 8 at%, the passivation elements of Zr and Ti increase from 55.5%, 12.2% to 62.2%, 15.3%, respectively, while the concentrations of Cu and Ni decrease from 14.7%, 9.4% to 6.9%, 6.3%, respectively. In other words, Zr and Ti elements are enriched with the increment of Nb content while the Cu concentration is decreased, which is in agreement with the results of Asami [13] and C. L. Qin [14], X. P. Nie [18].

As Cu is an unstable element in electrolyte open to the air and forms soluble porous Cu-Cl film, Cu is selectively corroded in priority and the content of Zr and Ti enriches after polarization. In our tests, Cu element is reduced with the increment of Nb content, which is consistent with the increment of pitting corrosion resistance. With Nb content increasing, the passivation region and pitting potential of BMG-coated steel wires increase while the corrosion current density decreases. As proposed by X. P. Nie[18], the metallic glass firstly decomposed into one Cu rich phase and one Zr and Nb rich phase, and then the Cu rich phase was selectively dissolved. So the change of alloy composition in pitting hole may correlate with the dual role as the addition of Nb. It is reported that the addition of Nb can stabilize Ti element which is easy to passivate in corrosion environment [14]. On one hand, Nb is a passivation film. On the other hand, Nb can stabilize

Table 1 Results of potentiodynamic polarization measurements for Q195 steel wire and $(Zr_{41.2}Ti_{13.8}Cu_{12.5}Ni_{10}Be_{22.5})_{100-x}Nb_x$ (x=0, 3, 5, 8)

Materials	Electrolyte	E_{corr}/mV	I_{corr}/mA cm^{-2}	E_{pit}/mV	E_{pit}–E_{corr}/mV
Q195 steel wire	3.56wt% NaCl	–650	1.87×10^{-2}		
Vit1 BMG-coated steel wire	3.56wt% NaCl	–409	3.71×10^{-4}	–268	141
(Vit1)97Nb3 BMG-coated steel wire	3.56wt% NaCl	–420	2.05×10^{-5}	–163	257
(Vit1)95Nb5 BMG-coated steel wire	3.56wt% NaCl	–459	8.06×10^{-5}	–148	311
(Vit1)92Nb8 BMG-coated steel wire	3.56wt% NaCl	–446	9.86×10^{-6}	–52	394

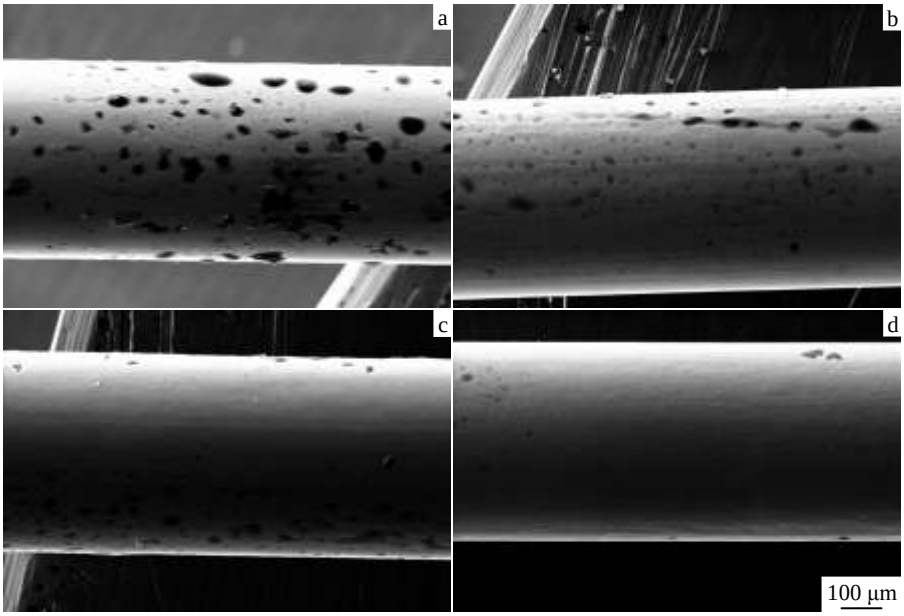

Fig.4 SEM images of the surface morphologies of $(Zr_{41.2}Ti_{13.8}Cu_{12.5}Ni_{10}Be_{22.5})_{100-x}Nb_x$ BMG-coated Q195 steel wires after potentiodynamic polarization tests at ambient temperature: (a) x=0, (b) x=3, (c) x=5, and (d) x=8

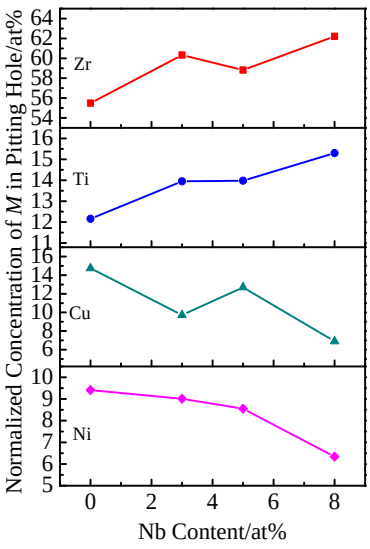

Fig.5 Normalized concentration of metal obtained from the EDS data in the pitting holes after potentiodynamic polarization tests

the two easily passivating elements of Zr and Ti to avoid formation of an element which is easy to passivate and form stable Cu rich phase and Zr and Ti rich phase. Thus, the number and concentration of Cu rich phase zones are reduced and more stable passivation films are formed with the increment of Nb, which is in agreement with the surface morphology change in Fig.4 and the alloy composition change of pitting hole in Fig.5. It should be also noticed that the $(Zr_{41.2}Ti_{13.8}Cu_{12.5}Ni_{10}Be_{22.5})_{95}Nb_5$-coated steel wire shows abnormal phenomena. In pitting holes of the $(Zr_{41.2}Ti_{13.8}Cu_{12.5}Ni_{10}Be_{22.5})_{95}Nb_5$-coated steel wire, the concentration of Zr element is lower than that of the $(Zr_{41.2}Ti_{13.8}Cu_{12.5}Ni_{10}Be_{22.5})_{97}Nb_3$-coated steel wire while the concentration of Cu element is higher than that of the $(Zr_{41.2}Ti_{13.8}Cu_{12.5}Ni_{10}Be_{22.5})_{97}Nb_3$-coated steel wire. It can be explained by that breaking the local passivation film, where the metallic glass coating contains crystalline phase NiZr, leads to the decrease of Zr and Ni elements. In other words, the decrease of Zr and Ni elements means the increment of Cu element in the pitting hole.

3 Conclusions

1) Compared with Q195 steel wires, $(Zr_{41.2}Ti_{13.8}Cu_{12.5}Ni_{10}Be_{22.5})_{100-x}Nb_x$ (x=0, 3, 5, 8, at%)-coated Q195 steel wires show a great improvement in corrosion resistance with a large passivation region, higher pitting potential and lower corrosion current density.

2) The resistance to pitting corrosion of metallic glass-coated steel wires increases with the increment of Nb content. The addition of Nb plays dual roles. On one hand, Nb is an element which is easy to passivate and form stable passivation film; on the other hand, Nb can stabilize the two easy passivating elements of Zr and Ti avoiding phase separation. Therefore the passivation region and pitting potential are increased with the increment of Nb content while corrosion current density is decreased.

References

1 Inoue A, Takeuchi A. *Acta Materialia*[J], 2011, 59(6): 2243
2 Ashby M F, Greer A L. *Scripta Materialia*[J], 2005, 54(3): 321
3 Greer A L, Ma E. *MRS Bulletin*[J], 2007, 32(8): 611

4 Peter W H, Buchanan R A, Liu C T *et al. Intermetallics*[J], 2002, 10(11-12): 1157
5 Huang L, Qiao C D, Green B A *et al. Intermetallics*[J], 2009, 17(4): 195
6 Vincent S, Khan A F, Murty B S *et al. Journal of Non-Crystalline Solids*[J], 2013, 379: 48
7 Inoue A, Zhang W, Zhang T *et al. Journal of Materials Research* [J], 2001, 16(10): 2836
8 Xie G Q, Qin F X , Zhu S L *et al. Intermetallics*[J], 2014, 44: 55
9 Zhu C L, Wang Q, Zhang J *et al. International Journal of Minerals, Metallurgy, and Materials*[J], 2010, 17(3): 323
10 Morrison M L, Buchanan R A, Peker A *et al. Intermetallics*[J], 2004, 12(10-11): 1177
11 Kamachi M U, Baunack S, Eckert J *et al. Journal of Alloys and Compounds*[J], 2004, 377(1-2): 290
12 Raju V R, Kühn U, Wolff U *et al. Materials Letters*[J], 2002, 57(1): 173
13 Asami K, Qin C L, Zhang T *et al. Materials Science and Engineering A*[J], 2004, S375-377: 235
14 Qin C L, Asami K, Zhang T *et al. Materials Transactions*[J], 2003, 44(4): 749
15 Jiang Q K, Qin C L, Amiya K *et al. Intermetallics*[J], 2008, 16(2): 225
16 Gebert A, Concustell A, Greer A L *et al. Scripta Materialia*[J], 2010, 62(9): 635
17 Gebert A, Gostin P F, Schultz L. *Corrosion Science*[J], 2010, 52(5): 1711
18 Nie X P, Xu X M, Jiang Q K *et al. Journal of Non-Crystalline Solids*[J], 2009, 355(3): 203
19 Zohdi H, Shahverdi H R, Hadavi S M M. *Electrochemistry Communications*[J], 2011, 13(8): 840
20 Huang Y J, Guo Y Z, Fan H B *et al. Materials Letters*[J], 2012, 89: 229
21 Kobayashi A, Yano S, Kimura H *et al. Materials Science and Engineering B*[J], 2008, 148(1-3): 110
22 Liu G , An Y, Guo Z *et al. Applied Surface Science*[J], 2012, 258(14): 5380
23 Wang Shanlin, Cheng Jingchang, Yi Seonghoon *et al. Transactions of Nonferrous Metals Society of China*[J], 2014, 24(1): 146
24 Zhang Zhibin, Liang Xiubing, Xu Binshi *et al. Rare Metal Materials and Engineering*[J], 2012, 41(S1): 872 (in Chinese)
25 Chu C W, Jang J S C, Chiu S M *et al. Thin Solid Films*[J], 2009, 517(17): 4930
26 Ningshen S, Kamachi Mudali U *et al. Surface & Coatings Technology*[J], 2011, 205(15): 3961
27 Kobayashi A, Kuroda T, Kimura H *et al. Materials Science and Engineering B*[J], 2010, 173(1-3): 122
28 Li C B, Chen D H, Chen W W *et al. Corrosion Science*[J], 2014, 84: 96
29 Li C B, Chen W W, Jiang Q S *et al. Materials Chemistry and Physics*[J], 2014, 143(3): 900
30 Kim J, Kang K, Yoon S *et al. Surface & Coatings Technology*[J], 2011, 205(8-9): 3020
31 Yu P, Chan K C, Xia L *et al. Materials Transactions, JIM*[J], 2009, 50(10): 2451
32 Chen X H, Zhang B Y, Chen G L *et al. Intermetallics*[J], 2010, 18(11): 2034
33 Chen X H, Zhang B Y, Chen G L *et al. Intermetallics*[J], 2011, 19(12): 1913
34 Zhang B Y, Chen X H, Wang S S *et al. Materials Letters*[J], 2013, 93(1): 210
35 Zhang B Y, Chen X H, Hui X D. *Journal of Alloys and Compounds*[J], 2013, 553(3): 14
36 Zhang B Y, Chen X H, Lu Z P *et al. International Journal of Minerals, Metallurgy, and Materials*[J], 2013, 20(5): 456
37 Chen X H, Zhang B Y, Hui X D. *International Journal of Minerals, Metallurgy, and Materials*[J], 2013, 20(6): 589

通过制备非晶涂覆钢丝提高钢丝抗腐蚀性能

张保玉[1]，郭新格[2]，陈晓华[3]，杨文智[1]，陈子明[1]，黄　伟[1]，尚福军[1]，史洪刚[1]

(1. 中国兵器科学研究院宁波分院，浙江 宁波 315103)

(2. 中国科学院固体物理研究所，安徽 合肥 230031)

(3. 北京科技大学 新金属材料国家重点实验室，北京 100083)

摘　要：为了提高钢丝的耐腐蚀性能，使用连续涂覆工艺制备一系列锆基非晶合金$(Zr_{41.2}Ti_{13.8}Cu_{12.5}Ni_{10}Be_{22.5})_{100-x}Nb_x$ (x=0, 3, 5, 8, at%)涂覆 Q195 钢丝。相分析结果表明，涂层主要由非晶基体和一些金属间化合物组成；阳极极化实验发现所有非晶涂覆钢丝表现钝化行为，具有高的点蚀破钝电位和低的腐蚀电流。随着非晶涂层中铌含量增加，非晶涂覆钢丝的钝化区宽度增加，点蚀破钝电位升高。电子能谱分析发现，非晶涂覆钢丝抗点蚀性能提升可能与金属铌元素容易钝化，形成稳定钝化膜，同时能够稳定锆、钛，降低相分离有关。

关键词：钢丝；金属玻璃；涂层；耐腐蚀性

作者简介：张保玉，男，1982 年生，博士，助理研究员，中国兵器科学研究院宁波分院，浙江 宁波 315103，电话：0574-87017901，E-mail: byzhang@outlook.com